HHS Public Access

Author manuscript

Exp Eye Res. Author manuscript; available in PMC 2016 September 01.

Published in final edited form as:

Exp Eye Res. 2015 September ; 138: 134–144. doi:10.1016/j.exer.2015.06.027.

REDUCTION OF AMYLOID-BETA LEVELS IN MOUSE EYE TISSUES BY INTRA-VITREALLY DELIVERED NEPRILYSIN

Rajni Parthasarathy[a,b], **K. Martin Chow**[c], **Zahra Derafshi**[b], **Michael P. Fautsch**[d], **John R. Hetling**[b], **David W. Rodgers**[c], **Louis B. Hersh**[c], and **David R. Pepperberg**[a,b,*]

[a]Lions of Illinois Eye Research Institute, Department of Ophthalmology and Visual Sciences, Illinois Eye and Ear Infirmary, University of Illinois at Chicago, Chicago, IL, USA

[b]Department of Bioengineering, University of Illinois at Chicago, Chicago, IL, USA

[c]Department of Molecular and Cellular Biochemistry, University of Kentucky, Lexington, KY, USA

[d]Department of Ophthalmology, Mayo Clinic, Rochester, MN, USA

Abstract

Amyloid-beta (Aβ) is a group of aggregation-prone, 38- to 43-amino acid peptides generated in the eye and other organs. Numerous studies suggest that the excessive build-up of low-molecular-weight soluble oligomers of Aβ plays a role in the progression of Alzheimer's disease and other brain degenerative diseases. Recent studies raise the hypothesis that excessive Aβ levels may contribute also to certain retinal degenerative diseases. These findings, together with evidence that a major portion of Aβ is released as monomer into the extracellular space, raise the possibility that a technology enabling the enzymatic break-down of monomeric Aβ in the living eye under physiological conditions could prove useful for research on ocular Aβ physiology and, perhaps ultimately, for therapeutic applications. Neprilysin (NEP), an endopeptidase known to cleave Aβ monomer into inactive products, is a membrane-associated protein. However, sNEP, a recombinant form of the NEP catalytic domain, is soluble in aqueous medium. With the aim of determining the Aβ-cleaving activity of exogenous sNEP in the microenvironment of the intact eye, we analyzed the effect of intra-vitreally delivered sNEP on ocular Aβ levels in mice that exhibit readily measurable, aqueous buffer-extractable $A\beta_{40}$ and $A\beta_{42}$, two principal forms of Aβ. Anesthetized 10-month wild-type (C57BL/6J) and 2–3-month 5XFAD transgenic mice received intra-vitreal injections of sNEP (0.004 – 10 μg) in one eye and were sacrificed at defined post-treatment times (30 min – 12 weeks). Eye tissues (combined lens, vitreous, retina, RPE and choroid) were homogenized in phosphate-buffered saline, and analyzed for $A\beta_{40}$ and $A\beta_{42}$ (ELISA) and for total protein (Bradford assay). The fellow, untreated eye of each mouse served as control, and concentrations of Aβ (pmol/g protein) in the treated eye were normalized to that of the untreated control eye. In C57BL/6J mice, as measured at 2 hr after sNEP treatment, increasing amounts of injected sNEP yielded progressively greater reductions of $A\beta_{40}$, ranging from 12% ±

*Corresponding author: Lions of Illinois Eye Research Institute, Department of Ophthalmology and Visual Sciences, University of Illinois at Chicago, 1855 W. Taylor St., Chicago, IL 60612, USA. Phone: +1 312 996 4262. davipepp@uic.edu.

3% (mean ± SEM; n=3) with 4 ng sNEP to 85% ± 13% (n=5) with 10 μg sNEP. At 4 ng sNEP the average $A\beta_{40}$ reduction reached >70% by 24 hr following treatment and remained near this level for about 8 weeks. In 5XFAD mice, 10 μg sNEP produced an $A\beta_{40}$ decrease of 99% ± 1% (n=4) and a substantial although smaller decrease in $A\beta_{42}$ (42% ± 36%; n=4) within 24 hr. Electroretinograms (ERGs) were recorded from eyes of C57BL/6J and 5XFAD mice at 9 days following treatment with 4 ng or 10 μg sNEP, conditions that on average led, respectively, to an 82% and 91% $A\beta_{40}$ reduction in C57BL/6J eyes, an 87% and 92% $A\beta_{40}$ reduction in 5XFAD eyes, and a 23% and 52% $A\beta_{42}$ reduction in 5XFAD eyes. In all cases, sNEP-treated eyes exhibited robust ERG responses, consistent with a general tolerance of the posterior eye tissues to the investigated conditions of sNEP treatment. The sNEP-mediated decrease of ocular Aβ levels reported here represents a possible approach for determining effects of Aβ reduction in normally functioning eyes and in models of retinal degenerative disease.

Keywords

amyloid-beta; neprilysin; intra-vitreal injection; C57BL/6J mouse; 5XFAD mouse; electroretinogram

1. INTRODUCTION

Amyloid-beta (Aβ) is a group of 38- to 43-amino acid peptides generated in the eye (Janciauskiene et al., 2011; Normando et al., 2009; Prakasam et al., 2010; Wang et al., 2011, 2012; Yoneda et al., 2005) and other organs. Aβ is formed via the sequential cleavage of amyloid precursor protein (APP) by β- and γ-secretases (Querfurth and LaFerla, 2010) and is released in monomeric form into the extracellular medium. $A\beta_{40}$ and $A\beta_{42}$, consisting of 40 and 42 amino acids, respectively, are among the most abundant forms of the peptide (Kummer and Heneka, 2014). $A\beta_{40}$ and particularly $A\beta_{42}$ undergo noncovalent oligomerization (aggregation) to form, progressively, soluble oligomers, insoluble fibrils and plaques (Benilova et al., 2012; Edwards et al., 2014; Johnson et al., 2002; Walsh and Selkoe, 2007), and exhibit intracellular uptake (LaFerla et al., 2007; Oddo et al., 2006; Ripoli et al., 2014). Aβ's functions are not fully understood (Benilova et al., 2012; Hubin et al., 2014; LaFerla et al., 2007; Oddo et al., 2006; Ripoli et al., 2014; Walsh and Selkoe, 2007). Multiple reports indicate a physiological role of the peptide in synaptic physiology (Abramov et al., 2009; Morley and Farr, 2014; Puzzo et al., 2008; Puzzo and Arancio, 2013) and as an anti-microbial agent (Soscia et al., 2010). However, numerous studies indicate that $A\beta_{42}$, and to a lesser extent $A\beta_{40}$, are cytotoxic for CNS neurons and microvascular endothelial cells (Bruban et al., 2011; Carvalho et al., 2014; Dahlgren et al., 2002; Itkin et al., 2011; Manzoni et al., 2011; Pauwels et al., 2012; Selkoe, 2012; Solomonov et al., 2012; Yankner and Lu, 2009). Recent data implicate, as a particularly toxic form of Aβ, relatively small soluble oligomers that represent initial states of the process of aggregation of Aβ monomers (Benilova et al., 2012; Luibl et al., 2006; Pryor et al., 2012; Warmlander et al., 2013).

Beyond a pathological role in brain degenerative diseases, excess Aβ has been hypothesized to exert toxic effects in posterior eye tissues and to play a role in retinal diseases such as age-related macular degeneration (Dentchev et al., 2003; Hoh Kam et al., 2010; Isas et al.,

2010; Liu RT et al., 2013; Liu Y et al., 2015; Ning et al., 2008). Multiple findings are consistent with direct and/or indirect effects of Aβ build-up in the progression of AMD. For example, large drusen at the RPE/Bruch's membrane interface, a hallmark of AMD, typically contain significant levels of aggregated Aβ (Isas et al., 2010; Johnson et al., 2002). Furthermore, known AMD risk factors including high-fat/high cholesterol diet, light damage, exposure to cigarette smoke and iron overload are associated with Aβ build-up (Beatty et al., 2000; Cano et al., 2010; Dasari et al., 2011; Ding et al., 2008, 2011; Dong et al., 2012; Guo et al., 2014; Malek et al., 2005; Organisciak and Vaughan, 2010; Pikuleva and Curcio, 2014; Sharma et al., 2014; Woodell and Rohrer, 2014). In addition, partial rescue/protection from retinal/RPE abnormalities in retinal degeneration mouse models can be achieved by Aβ-directed immunotherapy (Ding et al., 2008, 2011; Guo et al., 2007).

The numerous gaps in present understanding of Aβ's action in eye tissues, and the possibility that Aβ may promote retinal and RPE degeneration, raise interest in exploring experimental approaches that could enable control of Aβ levels in the living eye for investigational purposes and, potentially, for therapeutic applications. As noted, previous studies have shown that treatment with anti-Aβ antibodies mitigates ocular pathology induced by high fat/high cholesterol diet (Ding et al., 2008, 2011). To our knowledge, however, no one has tested the feasibility of reducing Aβ levels in the living eye by promoting its degradation. Given that nascent Aβ is a monomeric water-soluble molecule, and to a considerable extent is released into the extracellular medium, we reasoned that this early-arising form of Aβ might be readily susceptible to degradation by a soluble Aβ-cleaving enzyme delivered to the aqueous milieu of the eye. Neprilysin (EC 3.4.24.11), a widely distributed endopeptidase known to cleave Aβ monomers into inactive products (Hersh and Rodgers, 2008; Iwata et al., 2001; Nalivaeva et al., 2012), is a membrane-associated protein (Carson and Turner, 2002; Roques et al., 1993; Turner et al., 2001). However, recent work has shown that a recombinant soluble form of neprilysin (here termed "sNEP") containing the enzyme's catalytic domain retains Aβ-cleaving activity (Liu et al., 2010). Here we report that, in two mouse models chosen for their expression of readily measurable aqueous-extractable ocular Aβ (10-month C57BL/6J and 2–3 month 5XFAD mice), decreases in ocular Aβ under conditions that preserve good electroretinographic (ERG) responsiveness can be induced in a controlled, dose-dependent manner by the intra-vitreal delivery of sNEP.

2. METHODS

2.1. Animals

All procedures for animal handling were approved by the University of Illinois at Chicago's Institutional Animal Care and Use Committee (IACUC), and conformed to the statement on the use of animals in ophthalmic and vision research, established by the Association for Research in Vision and Ophthalmology (ARVO). C57BL/6J (i.e., wild-type) mice (1–2-months old; and 10-months old retired breeders) and 5XFAD mice (2–3-month old, product no. 034848, on a C57BL/6J background) were obtained from Jackson Laboratories (Bar Harbor, ME). The 5XFAD mouse, a transgenic strain that over-expresses a mutant form of APP 695 containing Swedish, Florida, and London familial Alzheimer's disease (FAD)

mutations as well as human PS1 harboring two FAD mutations, produces elevated levels of $A\beta_{42}$ (Alexandrov et al., 2011; Oakley et al., 2006; Park et al., 2014). Mice were maintained on a 12-hr light/12-hr dark cycle (~2–18 lux).

2.2. Intra-vitreal injection, post-injection maintenance period, and euthanasia

Mice were anesthetized (intra-peritoneal injection of ketamine and xylazine, 0.15 and 0.01 mg per g body weight, respectively) and positioned on a warming blanket throughout the period of anesthesia. Boosts of anesthetic (~1/6 of the initial dose) were delivered as previously described (Hetling and Pepperberg, 1999). Unless otherwise indicated, experiments investigating the action of test agents involved the treatment of one eye of a given animal; the fellow eye remained untreated and served as a control. The cornea was anaesthetized using 0.5 % proparacaine hydrochloride. Intra-vitreal injection was visualized with the use of an operating microscope. With the eye held in place in the orbit, a 32-gauge needle was used to puncture the superior nasal sclera at the pars plana. Test solutions (2 μL) were injected into the vitreal cavity using a glass capillary (with finely drawn tip) that was connected to a delivery syringe. Mice were maintained from 30 min up to 12 weeks following intra-vitreal treatment. In cases where the post-treatment maintenance period was ≤ 4 hr, animals were kept under anesthesia until euthanasia. For periods >4 hr, the mice were permitted to recover from anesthesia and were re-anesthetized shortly before euthanasia. Unless otherwise stated, 2 μL of a solution containing 1 mM of the sNEP inhibitor phosphoramidon (PA; Sigma-Aldrich, St. Louis, MO) was delivered intra-vitreally to the treated eye approximately 15 min before euthanasia (see Results). Euthanasia was performed by carbon dioxide asphyxiation and cervical dislocation.

2.3. Extract preparation

Unless otherwise indicated, analyses were performed on phosphate-buffered saline (PBS) extracts of combined eye tissues (combined lens, vitreous, retina, RPE and choroid). With the eye of the euthanized mouse still in the orbit, an incision was made in the cornea, and the tissues (excluding the cornea and sclera) were removed using forceps. The combined removed tissues were transferred to a 1 mL Dounce tissue homogenizer (Wheaton, Millville, NJ), to which was added 200 μL of PBS containing chelator-free protease inhibitor cocktail (Calbiochem, San Diego, CA). With the homogenizer positioned in an ice bath, the tissue was homogenized by 30 even strokes delivered manually over ~30 s. The homogenate was then transferred to an Eppendorf tube and centrifuged (12000 rpm, 15 min, 4°C) to pellet insoluble material. The recovered supernatant (approximately 200 μL) was withdrawn, transferred to a new tube, and stored at −20°C until further analysis.

2.4. Recovery/preparation of separate eye tissues

A procedure modified from that described in the main Methods section was used to separately recover three samples from the eye: lens/vitreous, neural retina, and RPE/choroid. Here, the intact eye was removed from the orbit, and an incision was made normal to the axis of the eye at a plane anterior to the limbus, leaving a small uncut segment. With forceps, the cornea was peeled back to expose the lens. With a fresh pair of tweezers, the lens and adhering vitreous were removed and transferred to a tube containing 200 μL of ice-cold PBS (sample A). In cases where a visible amount of vitreous remained in the eye, the

remaining vitreous was withdrawn into a syringe and combined with the previously removed lens and vitreous. Next, the neural retina was gently separated from the RPE at all locations except for the optic nerve head. The retina was then removed by snipping the optic nerve immediately beneath the retina, and transferred to 200 μL of ice-cold PBS (sample B). Finally, while stabilizing the globe via the remaining corneal flap, the RPE and choroid were together removed using forceps and transferred to 200 μL of ice-cold PBS (sample C). Samples A, B and C were then homogenized and the PBS extract analyzed as described for the combined-tissue extract.

2.5. sNEP preparation

sNEP was generated in the *Pichia* yeast system (Invitrogen, Carlsbad, CA) as previously described (Dale et al., 2000). Briefly, the α-factor secretion signal and a poly-histidine affinity tag were fused to the *N*-terminus of the extracellular domain of NEP, yielding secretion of the His-tagged sNEP into the media. The enzyme was precipitated from conditioned YP medium with ammonium sulfate at 55–70% saturation, dialyzed against Buffer A (20 mM potassium phosphate buffer, pH 7.7, plus 300 mM NaCl), and affinity-purified with a HIS-select nickel resin (Sigma-Aldrich) in a 15-mL column. After washing the column with Buffer A, sNEP was eluted with 150 mM imidazole in Buffer A, dialyzed against PBS and concentrated with a Millipore concentrator. The soluble NEP was homogeneous as determined by SDS-PAGE (Fig. 1), and retained full enzymatic activity.

2.6. ELISA

Aβ levels in the extracts were quantified using commercial ELISA kits. The ELISA kit for $A\beta_{40}$ (SIG-38954; Covance, Dedham, MA) detects both mouse and human $A\beta_{40}$. That for $A\beta_{42}$ (80177; Innogenetics; Ghent, Belgium) detects only human $A\beta_{42}$. Standard curves for $A\beta_{40}$ and $A\beta_{42}$ were determined in all experiments using standards provided by the manufacturers. Unless otherwise stated, ELISA determinations of Aβ in the extract of each eye were based on data obtained from ≥ 2 replicate samples. For both $A\beta_{40}$ and $A\beta_{42}$, the Aβ concentration in a given ELISA well was taken as below detection if the raw absorbance reading was less than 20% greater than the reading obtained from the blank well. Statistical significance was tested by two-tailed Student's t-test analysis. Error intervals reported for ELISAs and all other biochemical data represent SEM values.

2.7. Protein

Protein levels in eye tissue extracts were determined using the Bradford assay with bovine serum albumin as standard. Unless otherwise stated, Aβ concentrations are expressed as pmol Aβ per gram protein (pmol/g) contained in the parent tissue extract.

2.8. sNEP activity and level

sNEP activity was determined in a continuous couple assay using the substrate glutaryl-Ala-Ala-Phe-methoxynaphthylamine (GAAF-MNA) (Li and Hersh, 1995). The amount of activity remaining after defined post-treatment periods was expressed relative to the amount of activity injected into the eye. Western blot analysis of tissue homogenates was performed using a goat-anti-NEP polyclonal antibody (R&D Systems, Minneapolis, MN) as the

primary antibody and anti-goat HRP (Invitrogen) as the secondary antibody. Visualization was performed using a ChemiDoc™ MP imaging system (Bio-Rad Laboratories, Inc., Hercules, CA).

2.9. Electroretinography (ERG recording)

ERG responses were recorded from mice that had been dark-adapted for approximately 3 hr. ERGs were recorded from the eye that had been treated with sNEP or with PBS. Procedures used for anesthesia, animal temperature control, and ERG recording were similar to those previously described (Hetling and Pepperberg, 1999). Stimuli were generated by a xenon flash lamp (standard flash head; Novatron, Inc., Dallas, TX). Light passed through an adjustable aperture (to control luminance), a heat filter (Schott KG-3; Phillips Safety Products, Middlesex, NJ), and diffusers prior to backlighting a translucent full-field viewing surface. Flash strengths ranged from 0.04 to 8.33 sc cd s m^{-2} (scotopic candela seconds per meter squared) (IL-1700 photometer; International Light, Inc., Newburyport, MA). Responses were sampled at 5 kHz, filtered with a pass band of 0.2 Hz – 2.5 kHz, and stored for later analysis. The mice were euthanized at 2–6 hr after ERG recording (no PA treatment was included in these experiments) and analyzed for relative levels of $A\beta_{40}$ and, for the 5XFAD mice, $A\beta_{42}$.

2.10. Vitreous samples from human donor eyes

The use of human donor eyes was approved by the Mayo Clinic and the University of Illinois at Chicago Institutional Review Boards, and conformed to the Declaration of Helsinki. Vitreous humor was isolated in Dr. Fautsch's laboratory from 14 eyes obtained from 7 donors (age range: 55 to 101 years) within 12.5 ± 2.0 hr of death (range 4.5–18 hr). Vitreous was stored at −80°C and subsequently shipped on dry ice to Dr. Pepperberg's laboratory for analysis. Analyses were carried out on two 400-μL aliquots of vitreous obtained from each of the 14 eyes. To assess the effect of sNEP, each 400-μL aliquot received either 4 μL of PBS that contained 20 μg of sNEP (test samples) or 4 μL of PBS alone (control samples). The samples were incubated at 37°C for 20 min, further supplemented with 4 μL of 10 mM PA, and then analyzed for $A\beta_{40}$, $A\beta_{42}$, and total protein. ELISA determinations were based on data obtained from two replicates of each sample.

3. RESULTS

3.1. Abundance of Aβ in untreated eyes

10-month C57BL/6J mice and 2–3-month old 5XFAD mice exhibit readily measurable nominal levels of ocular Aβ. Table 1 shows determinations of $A\beta_{40}$ and $A\beta_{42}$ levels in combined-tissue extracts of eyes of 10-month C57BL/6J and 2–3-month 5XFAD mice. These eyes were untreated, i.e., did not receive additions of sNEP or any other agent. In C57BL/6J mice, the concentration of $A\beta_{40}$ in 10-month animals differed significantly from that in 2-month animals ($p<0.001$) and was, on average, more than 15 times as great as that in 2-month animals. Two-to-three-month old 5XFAD mice exhibited an average $A\beta_{40}$ level almost twice that of the 10-month C57BL/6J mice, and this presumably represented a mixture of endogenous mouse $A\beta_{40}$ and human transgenic $A\beta_{40}$. The level of $A\beta_{42}$ in 2–3-month old 5XFAD mice, which represented ~20% of the $A\beta_{40}$ level (significantly lower

than the $A\beta_{40}$ level; $p<0.001$), reflected only transgene expression, as the Innotest anti-$A\beta_{42}$ antibody used in this study was specific for human $A\beta_{42}$. Extraction of eye tissues from untreated 10-month C57BL/6J and 2–3-month 5XFAD eyes using PBS supplemented with 1% v/v Triton-X (and subsequent protein analysis using the BCA assay) yielded results that did not differ substantially from those obtained with PBS alone (data not shown).

3.2. Overall design of sNEP experiments

We sought an experimental design through which the Aβ-cleaving activity of intra-vitreally delivered sNEP could be determined by the analysis of eye tissue from a single mouse. To compensate for inter-animal variability in absolute concentrations of Aβ in the eye tissues, we adopted, as a standard procedure, the delivery of sNEP to one eye of the animal under study while the fellow eye served as untreated control. As the primary parameter by which to characterize sNEP activity, we determined *relative Aβ,* defined as the ratio of Aβ concentration (pmol Aβ per g protein) in the extract of the treated eye divided by the Aβ concentration in the fellow, untreated eye. Because of the tiny mass of mouse eye tissues, and the anticipated diffusion of both aqueous-extractable Aβ and sNEP among different eye compartments during tissue recovery, the experiments routinely employed the recovery of combined lens, vitreous, retina and RPE choroid.

3.3. sNEP activity in C57BL/6J mice

We first investigated changes in $A\beta_{40}$ level produced by intra-vitreal treatment only with sNEP, i.e., with no subsequent *in vivo* delivery of any agent to the test eye of the animal. Fig. 2A shows results obtained when the treatment with sNEP (0.04 or 12 μg) was followed by a 2-hr period of animal maintenance, and then euthanasia and tissue extraction/analysis. Mice that in one eye received PBS vehicle alone served as controls. As illustrated, values of relative $A\beta_{40}$ indicated large reductions of $A\beta_{40}$ in the sNEP-treated eyes, with no significant effect of PBS treatment on Aβ levels.

Although the Fig. 2A data are consistent with *in vivo* $A\beta_{40}$ degradation by the intra-vitreally delivered sNEP, the post-euthanasia time period and procedures (eye tissue removal, homogenization, extraction, and ELISA analysis) required for Aβ quantification left open the possibility that sNEP activity persisting in the harvested tissues contributed significantly to the measured Aβ reduction. To minimize the contribution of possible neprilysin-mediated Aβ cleavage following euthanasia, we adopted, as an element of the standard procedure, the intra-vitreal delivery of phosphoramidon (PA), a potent and relatively specific inhibitor of NEP activity (Hersh and Rodgers, 2008; Li and Hersh, 1995; Shirotani et al., 2001), at ~15 min before euthanasia. As illustrated in Fig. 2B, at lower sNEP doses (0.004 and 0.04 μg), extracts from PA-treated eyes (filled circles) exhibited Aβ reductions significantly less extensive ($p<0.05$) than those of eyes not receiving PA (open circles). In a separate experiment (not illustrated), we pre-incubated PA (2 μL of 100 μM) with sNEP (10 μg in 2 μL PBS), delivered 2 μL of the mixture intra-vitreally, and maintained the mice for 2 hr before euthanasia. With use of this sNEP/PA mixture, there was no significant $A\beta_{40}$ reduction (relative $A\beta_{40}$ in the treated eyes: 0.96 ± 0.20; $n=2$; $p = 0.71$), indicating that PA's presence at the time of intra-vitreal sNEP delivery eliminated sNEP's *in vivo* activity. Furthermore, PA alone (2 μL of 1 mM) delivered at the beginning of a 2-hr maintenance

period had no significant effect on relative Aβ level in the treated eye (1.00 ± 0.14; n = 3; p = 0.92; not illustrated), indicating that there were no other PA-sensitive proteases degrading Aβ. Together, the results provided evidence for the desirability of including PA treatment, particularly under conditions of relatively low sNEP dose and brief (2-hr) post-treatment period. Intra-vitreal delivery of PA (2 μL of 1 mM) ~15 min before euthanasia was therefore adopted as a routine procedure (Fig. 2C). More generally, the data of Fig. 2B demonstrate a robust, relatively simple relationship between sNEP dose and $A\beta_{40}$ reduction that at the highest investigated dose (10 μg) achieves near-complete $A\beta_{40}$ cleavage within 2 hr.

Fig. 3 illustrates the time course of changes in relative $A\beta_{40}$ levels produced by a fixed dose of sNEP (4 ng). With post-treatment periods of 30 min and 2 hr, this low dose of sNEP did not reduce $A\beta_{40}$ levels significantly. However, relative $A\beta_{40}$ was decreased substantially at 24 hr post-treatment, and the attained low level (~0.3, on average) persisted for post-treatment periods of up to 8 weeks. At 12 weeks post-treatment, relative Aβ remained below unity but significantly exceeded that exhibited at 8 weeks, indicating replenishment of the ocular Aβ pool.

The prolonged sNEP-induced Aβ reduction likely reflects the absence of substantial net Aβ formation during the post-treatment period, or the cleavage of newly generated Aβ by remaining sNEP activity. To obtain information on this point, we treated one eye of each of 6 C57BL/6J mice with 10 μg of sNEP and, following post-treatment periods that omitted PA delivery, determined the amount of remaining sNEP activity relative to the amount of activity injected into the mouse eye (fluorometric assay; Fig. 4A) and of sNEP protein (Western blot; Fig. 4B). The activity data showed that after 2 hr, more than 50% of the sNEP was degraded and/or cleared from the eye. By 48 hr, there was no detectable sNEP activity (Fig. 4A) or protein (Fig. 4B).

3.4. sNEP activity in 5XFAD mice

In experiments similar to those of Fig. 3, we examined the effect of intra-vitreal sNEP treatment in a relatively small number of 2–3 month 5XFAD mice that were available for this study. The occurrence of readily measurable nominal levels of both $A\beta_{40}$ and $A\beta_{42}$ in these animals (Table 1) enabled analysis of the effects of sNEP treatment on both forms of Aβ. Table 2 shows results obtained in experiments that involved the variation of intra-vitreally delivered sNEP dose and post-treatment period. A prominent feature of the data shown in the Table concerns the relative reductions in $A\beta_{42}$ *vs.* $A\beta_{40}$ determined under a given experimental condition; that is, under each of these conditions, the reduction in relative $A\beta_{40}$ significantly ($p<0.04$) exceeded that for $A\beta_{42}$. The relationships between relative extents of reduction were particularly pronounced with brief (2-hr) treatment at even high sNEP dose (10 μg), where $A\beta_{42}$ reduction was not significant but $A\beta_{40}$ reduction was 89% ± 9%. Data obtained with the same high dose of sNEP and longer post-treatment periods indicated near-complete $A\beta_{40}$ reduction. By contrast, post-treatment periods spanning 1 day to 1 month yielded an apparent plateau of $A\beta_{42}$ reduction amounting, on average, to roughly 50%. $A\beta_{42}$ reductions were themselves substantial under conditions other than those involving short (2-hr) post-treatment with 10 μg sNEP or 1-day post-treatment with low-dose sNEP. Relative $A\beta_{40}$ at 1 month, while low (0.15 ± 0.02), was

significantly greater than that at 1 and 3 days ($p<0.05$). These data show that ~50% of the ELISA-detectable $A\beta_{42}$ recovered from the eye appears resistant to cleavage by sNEP. However, the data do not establish the extent to which this sNEP-resistant fraction consists of soluble oligomeric $A\beta_{42}$ which is not cleaved by sNEP (see Discussion).

3.5. Aβ in separate eye compartments

As noted above, the standard procedure used in the experiments involved the recovery of combined eye tissues from untreated and sNEP-treated eyes. However, we conducted additional experiments that involved the recovery/analysis of separate lens/vitreous, neural retina, and RPE choroid.

Nominal Aβ levels—We determined the levels of $A\beta_{40}$ and $A\beta_{42}$ in separately recovered lens/vitreous, retina, and RPE/choroid of 10-month C57BL/6J and 2–3-month 5XFAD mice. The concentrations of $A\beta_{40}$ associated with these separate compartments of C57BL/6J eyes (Table 3) were of similar order of magnitude. Furthermore, the sum of concentrations determined for these compartments did not differ significantly from that determined in the combined-tissue extracts (cf. Table 1) ($p>0.1$). Table 3 shows the results obtained. For C57BL/6J mice, protein-normalized levels of $A\beta_{40}$ (rows 1–3) did not differ significantly from one another ($p>0.05$), and the sum of levels determined in the 3 compartments (43.8 ± 6.9) did not differ significantly from the $A\beta_{40}$ levels determined in the combined-tissue samples of Table 1 ($p>0.1$). For the 5XFAD mice, there were no significant differences among the separate compartment determinations for either $A\beta_{40}$ ($p>0.05$) or $A\beta_{42}$ ($p>0.1$) (Table 3, rows 4–6), and the summed levels for both $A\beta_{40}$ and $A\beta_{42}$ (63.8 ± 20.1 for $A\beta_{40}$; 28.2 ± 15.3 for $A\beta_{42}$) did not differ significantly from the Table 1 combined-tissue determinations ($p= 0.57$ for $A\beta_{40}$; $p= 0.21$ for $A\beta_{42}$). Thus, the concentrations of $A\beta_{40}$ and $A\beta_{42}$ determined for combined-tissue extracts (Table 1) reflected measurable contributions from each of the three compartments described in Table 3.

Effect of sNEP treatment—Fig. 5 shows relative concentrations of Aβ remaining in separately isolated lens/vitreous, retina, and RPE/choroid following delivery of 10 μg sNEP to one eye of each animal and a 24-hr post-treatment period. In C57BL/6J mice, sNEP treatment produced significant reductions in $A\beta_{40}$ in the three compartments, i.e., post-treatment relative levels of $A\beta_{40}$ in each differed significantly from unity ($p<0.05$) (Fig. 5A). $A\beta_{40}$ reduction in the retina also exceeded that in the lens/vitreous, despite the greater nominal concentration of $A\beta_{40}$ in the retina *vs*. lens/vitreous of untreated eyes (Table 3; 16.2 ± 2.9 *vs.* 8.2 ± 2.2 pmol/g, respectively). Aβ reduction in the retina also exceeded that in the RPE/choroid. In sNEP-treated 5XFAD mice, relative $A\beta_{40}$ significantly differed from unity in all three compartments, and reductions for $A\beta_{40}$ exceeded those for $A\beta_{42}$ in each (Fig. 5B), consistent with the finding (Table 2) of relatively more extensive $A\beta_{40}$ reduction in combined-tissue extracts from sNEP-treated 5XFAD eyes.

3.6. sNEP-mediated cleavage of $A\beta_{40}$ and $A\beta_{42}$ *in vitro*

To assess the relative activity of sNEP in cleaving $A\beta_{40}$ *vs*. $A\beta_{42}$ *in vitro*, we used purified sNEP and ensured that all of the $A\beta_{42}$ was soluble by dissolving the $A\beta_{42}$ in 1,1,1,3,3,3-hexafluoro-2-propanol, drying the sample, and then dissolving the $A\beta_{42}$ in buffer

immediately before its use. The hydrolyses of $A\beta_{40}$ and $A\beta_{42}$ by purified sNEP were determined using 10 μM Aβ incubated with sNEP in 25 mM potassium phosphate buffer, pH 7.5 at 37 °C. The amount of remaining peptide was determined by reversed-phase HPLC as a function of time (Liu et al., 2007). The determined rate of hydrolysis for $A\beta_{42}$ was 2.1 μmol/min per mg sNEP. We observed that, when incubated alone, there was a non-enzymatic loss of $A\beta_{42}$, ~5% loss in 20 min and ~10% loss in 40 min, presumably due to oligomerization. Therefore, reactions were not incubated for more than 20 min and the observed reaction rate was corrected for the non-enzymatic loss. For $A\beta_{40}$, no time-dependent loss of peptide was observed. The measured rate of $A\beta_{40}$ hydrolysis was 5.3 μmole/min per mg sNEP. Thus, the sNEP cleavage rate for $A\beta_{40}$ was approximately 2.5 times that for $A\beta_{42}$. This 2.5-fold difference is further minimized, since the Km for $A\beta_{40}$ is 1.6 times that for $A\beta_{42}$ (Shirotani et al., 2001).

3.7. Electroretinography

The evidence that intra-vitreally delivered sNEP can readily decrease ocular Aβ levels *in vivo* directs interest to the broad question of how such treatment affects the status of the eye tissues. As an initial step toward addressing this broad issue, we examined sNEP-treated eyes for ERG responsiveness as a measure of retinal function. For these experiments we selected both a relatively low (0.004 μg) and a relatively high (10 μg) dose of sNEP, and a single post-treatment period (9 days) over which both doses were anticipated to yield substantial Aβ reduction (Figs. 2–3 and Table 2). Fig. 6 shows results obtained in experiments conducted on a total of six 10-month C57BL/6J mice (Columns A–C) and six 2–3-month 5XFAD mice (Columns D–F). The tabular data shown in the lower portion of the Figure indicate the extents of Aβ reduction prevailing on the day of ERG recording. The Fig. 6 results show that treatment with both sNEP doses preserved overall robust ERG responsiveness. These results, while not addressing possible mechanisms that may link sNEP-induced Aβ changes with alterations in retinal function, indicate a general tolerance of the posterior eye tissues to sNEP treatment under the investigated conditions, and support the feasibility of ERG experiments that investigate this topic.

3.8. sNEP activity in vitreous of human donor eyes

Human vitreous is known to contain $A\beta_{40}$ and $A\beta_{42}$ (Parthasarathy et al., 2014; Prakasam et al., 2010; Yoneda et al., 2005). As a test of sNEP's activity on native $A\beta_{40}$ and $A\beta_{42}$ present in the human eye, we determined levels of $A\beta_{40}$, $A\beta_{42}$ and protein in human vitreous samples from 14 eyes (7 donors) that were supplemented with sNEP or with PBS alone. Data obtained from the PBS-treated samples indicated the presence of 126.6 ± 57.3 pmol/g $A\beta_{40}$ and 15.6 ± 5.7 pmol/g $A\beta_{42}$. For the pair of vitreous samples obtained from each donor, we tested for a significant difference between the Aβ levels determined for the left- and right-eye samples. As shown in Table 4, none of the left-eye *vs*. right-eye determinations for $A\beta_{40}$ showed a significant difference ($p<0.05$) by t-test; for $A\beta_{42}$, only in the case of one donor (donor 2) was there a significant difference. For the sNEP-treated samples, relative levels of $A\beta_{40}$ and $A\beta_{42}$ (pmol Aβ per g protein in the sNEP-treated sample normalized to that of the PBS-supplemented control sample) were, respectively, 0.46 ± 0.10 and 0.67 ± 0.14; these determinations differed significantly from unity ($p<0.001$). The distribution of results obtained from PBS- *vs*. sNEP-supplemented vitreous samples is

shown in Fig. 7, which plots the levels (pmol/g) of $A\beta_{40}$ (panel A) and $A\beta_{42}$ (panel B) as a function of donor age. There was no obvious relationship between donor subject age and the absolute Aβ concentration.

4. DISCUSSION

The results show that sNEP, the catalytically active domain of NEP, exhibits robust activity in reducing endogenous ocular Aβ when delivered intra-vitreally into the living eye of the mouse. Specifically, in 10 month C57BL/6J mice, intra-vitreal delivery of 4 ng sNEP reduces $A\beta_{40}$ by 78% ± 14% within 24 hr as determined in combined-tissue extracts (Fig. 3). Significant sNEP-mediated Aβ reductions are evident also in data obtained from separated lens/vitreous, retina, and RPE/choroid (Fig. 5). In 5XFAD mice, and as determined in combined-tissue extracts, 4 ng sNEP decreases $A\beta_{40}$ by 62% ± 1% within a 24-hr period, an extent similar to that exhibited in C57BL/6J mice. However, in 5XFAD mice, a significant reduction in $A\beta_{42}$ at 24 hr requires a higher sNEP dose (5 μg) (Table 2). Overall, the data obtained from combined and separate eye tissue extracts indicate that a substantial portion of Aβ in the mouse eye is accessible to cleavage by intra-vitreally introduced sNEP.

The present study does not establish how the activity of intra-vitreally introduced sNEP compares with the activity of NEP that may be present endogenously in mouse eye tissues. For example, the PBS extraction procedure used in the enzymatic activity and Western blot experiments of Fig. 4 would not have recovered endogenous membrane-associated NEP. That endogenous NEP activity is relatively low in the C57BL/6J mice investigated here comes from control experiments that involved intra-vitreal treatment with PA. We found that for mice treated with PA alone in one eye, the relative $A\beta_{40}$ level normalized to that of the fellow untreated eye did not differ significantly from unity (see Results text). Here, the presence of substantial endogenous NEP activity in the untreated control eye would have yielded a relative $A\beta_{40}$ level greater than unity. Overall, while there is ample evidence for NEP expression in CNS neurons, little information is available specifically on endogenous NEP activity in eye tissues.

A noteworthy feature of sNEP-mediated $A\beta_{40}$ reduction in 10-month C57BL/6J mice is the persistence of this effect over an 8-week period (Fig. 3). This contrasts with the indication (Fig. 4) of inactivation or removal of essentially all of delivered sNEP within ~48 hr after intra-vitreal delivery. While the Fig. 3 data are consistent with a near-absence of $A\beta_{40}$ generation or very slow net accumulation of Aβ during the 8-week period, other possibilities are not ruled out. One such possibility is that the low level of $A\beta_{40}$ maintained for weeks after sNEP treatment reflects a persisting substantial rate of Aβ cleavage by an undetectably low level of residual sNEP. An alternative possibility is that the accumulation of Aβ with age (cf. Table 1) reflects a developing disparity between the generation and the degradation/clearance of Aβ (Bates et al., 2009; Nalivaeva et al., 2012; Wildsmith et al., 2013), but that, upon the marked decrease in Aβ induced by sNEP treatment, endogenous Aβ degradation/clearance processes (Saido and Leissring, 2012; Tanzi et al., 2004; Yoon and Jo, 2012) become able to maintain Aβ at relatively low levels for many weeks.

The present findings raise multiple interesting questions whose resolution will be important for evaluating the usefulness of sNEP-mediated Aβ reduction as an investigative tool and, perhaps ultimately, as an approach for mitigating Aβ toxicity in retinal disease. One class of questions concerns the effect of sNEP treatment on the overall abundance of Aβ in the eye tissues. That is, there is ample evidence that Aβ (in particular $A\beta_{42}$) undergoes aggregation to form soluble oligomers, and insoluble fibrils and plaques (see Introduction). However, neprilysin degrades monomers. It has been reported to act relatively slowly on dimers and trimers (Hersh and Rodgers, 2008), which likely reflects the dissociation of oligomers into monomers, since the active site of NEP cannot accommodate even a dimer of Aβ (also, see Results section 3.6). Furthermore, the lesser relative activity of sNEP seen with $A\beta_{42}$ (Fig. 5B, Table 2) is likely due to $A\beta_{42}$'s propensity to aggregate (Benilova et al., 2012; Edwards et al., 2014; Johnson et al., 2002; Walsh and Selkoe, 2007) and/or the possibility of sequestration of such aggregates in cellular compartments (Burdick et al., 1997) that make it inaccessible and/or resistant to degradation by sNEP. Thus, under conditions of age and/or pathology associated with a substantial level of Aβ-containing deposits in the posterior eye tissues, sNEP treatment might lack significant effect on the overall quantity of Aβ, in particular, $A\beta_{42}$, and fail to mitigate pathological effects specifically due to the presence of these pre-formed aggregates.

A noteworthy further question raised by the observed effects of sNEP on the apparent change in relative $A\beta_{40}$ *vs*. $A\beta_{42}$ (Table 2; specifically the sNEP-resistant fraction referred to above) is whether sNEP treatment promotes an increase in the ratio of monomeric $A\beta_{42}$ to $A\beta_{40}$. Previous studies have provided evidence that interactions of $A\beta_{40}$ with $A\beta_{42}$ reduce the rate/extent of $A\beta_{42}$ aggregation (Pauwels et al., 2012; Gu and Guo, 2013). In this context, the observed greater extent of sNEP-mediated $A\beta_{40}$ reduction (Table 2) might be interpreted as promoting toxicity via an increase in the $A\beta_{42}/A\beta_{40}$ monomer ratio. However, the Table 2 data are consistent with the likelihood that sNEP-resistant $A\beta_{42}$ largely represents extracted, pre-existing $A\beta_{42}$ oligomers that contribute to the read-out signal in the ELISA assay. The nearly complete cleavage of monomeric $A\beta_{40}$ produced by a high dose of sNEP (Table 2) is accompanied by a comparable reduction in monomeric $A\beta_{42}$ if one corrects the end-point due to the sNEP-resistant $A\beta_{42}$. The present results obtained for the activity of sNEP *in vitro*, which show a relatively modest (2.5-fold or less) difference in sNEP-mediated cleavage of $A\beta_{40}$ vs. $A\beta_{42}$ (Results section 3.6), are consistent with this conclusion.

Despite the likelihood that intra-vitreally delivered sNEP leads to cleavage only of the monomeric forms of $A\beta_{40}$ and $A\beta_{42}$, sNEP-dependent reduction in these monomers, from which putatively highly toxic soluble oligomers as well as higher insoluble aggregates arise, could enable reduction or retardation of the formation, and thus pathological effects, of these large aggregates. Thus, for example, in an ultimate application to human eye diseases such as AMD, sNEP treatment initiated at an early disease stage might diminish Aβ accumulation in drusen at the RPE/BrM interface (Dentchev et al., 2003; Isas et al., 2010; Johnson et al., 2002; Luibl et al., 2006), and thus retard disease progression. The present results obtained from RPE/choroid recovered from sNEP-treated eyes (Fig. 5B), while representing an initial observation in a mouse model, raises interest in this long-term possibility.

A second group of questions in need of investigation relates to the substrate specificity of sNEP. While Aβ is a principal substrate of neprilysin, the enzyme is known to exhibit endopeptidase activity on peptides including insulin, bradykinin and substance P (Nalivaeva et al., 2012; however, see Liu et al., 2010). These non-Aβ activities suggest needed caution that unwanted side effects of sNEP treatment could complicate or compromise the investigational as well as therapeutic value of sNEP treatment.

Beyond its primary focus on determinations of sNEP-mediated Aβ-cleavage, the present study provides initial information on ERG responsiveness of sNEP-treated eyes. The data of Fig. 6 indicate a good tolerance to sNEP treatment, i.e., preservation of robust responsiveness, following treatments that substantially reduce $A\beta_{40}$ and $A\beta_{42}$ from their nominal levels. That is, the delivery of sNEP at the tested levels does not lead to an immediate catastrophic failure of retinal function. This result suggests the feasibility of ERG monitoring (along with other measures such as histological and immunological analysis) in future studies of the effects of sNEP treatment.

The ability of sNEP treatment to produce controlled reductions of ocular Aβ *in vivo* may enable progress in understanding the mechanisms underlying inter-relationships between Aβ build-up and retinal disease risks such as oxidative stress and other environmental factors such as high fat/high cholesterol diet (Ding et al., 2008, 2011). Conceivably, for example, animal studies involving oxidative challenge with *vs*. without sNEP treatment could yield information relevant to understanding, in the human eye, the extent to which Aβ dysregulation contributes to cellular and molecular changes promoted by oxidative stress. These investigational studies, if suggesting an ameliorating effect of sNEP-induced Aβ reduction, would raise interest in the possibility that the intra-ocular delivery of sNEP, the induced expression of the enzyme (Liu et al., 2009, 2010) in the eye tissues, or the secretion of sNEP by an implanted device (Lee et al., 2012; Tao, 2006) could have therapeutic potential in eye diseases that involve Aβ toxicity.

Acknowledgments

We thank Ms. Tara Nguyen for expert technical assistance with intra-vitreal injections, Ms. Cindy K. Bahler for isolation of human vitreous, Dr. Scott M. Plafker for helpful discussions, and Dr. Douglas L Feinstein and Mr. David J. Braun for providing mouse eye tissues used in early experiments. Supported by grants from the BrightFocus Foundation (Clarksburg, MD), the Illinois Society for the Prevention of Blindness (Chicago, IL), Research to Prevent Blindness (New York, NY) [Lew R. Wasserman Merit Award to Dr. Fautsch, and unrestricted awards to the University of Illinois at Chicago (UIC) Department of Ophthalmology and Visual Sciences and to the Department of Ophthalmology at Mayo Clinic], award UL1RR029879 from the UIC Center for Clinical and Translational Science (CCTS), and NIH grants EY001792, EY023430, EY021727 and GM110787.

Abbreviations

Aβ	amyloid-beta
NEP	neprilysin
sNEP	soluble catalytic domain of neprilysin
PA	phosphoramidon
ERG	electroretinogram

PBS	phosphate-buffered saline
RPE	retinal pigment epithelium
APP	amyloid precursor protein

References

Abramov E, Dolev I, Fogel H, Ciccotosto GD, Ruff E, Slutsky I. Amyloid-β as a positive endogenous regulator of release probability at hippocampal synapses. Nature Neurosci. 2009; 12:1567–1576.10.1038/nn.2433 [PubMed: 19935655]

Alexandrov PN, Pogue A, Bhattacharjee S, Lukiw WJ. Retinal amyloid peptides and complement factor H in transgenic models of Alzheimer's disease. Neuro Report. 2011; 22:623–627.10.1097/WNR.0b013e3283497334

Bates KA, Verdile G, Li QX, Ames D, Hudson P, Masters CL, Martins RN. Clearance mechanisms of Alzheimer's amyloid-beta peptide: implications for therapeutic design and diagnostic tests. Mol Psychiatry. 2009; 14:469–486.10.1038/mp.2008.96 [PubMed: 18794889]

Beatty S, Koh H-H, Phil M, Henson D, Boulton M. The role of oxidative stress in the pathogenesis of age-related macular degeneration. Surv Ophthalmol. 2000; 45:115–134.10.1016/S0039-6257(00)00140-5 [PubMed: 11033038]

Benilova I, Karran E, De Strooper B. The toxic Aβ oligomer and Alzheimer's disease: an emperor in need of clothes. Nature Neurosci. 2012; 15:349–357.10.1038/nn.3028 [PubMed: 22286176]

Bruban J, Maoui A, Chalour N, An N, Jonet L, Feumi C, Tréton J, Sennlaub F, Behar-Cohen F, Mascarelli F, Dinet V. CCR2/CCl2-mediated inflammation protects photoreceptor cells from amyloid-β-induced apoptosis. Neurobiol Dis. 2011; 42:55–72.10.1016/j.nbd.2011.01.004 [PubMed: 21220018]

Burdick D1, Kosmoski J, Knauer MF, Glabe CG. Preferential adsorption, internalization and resistance to degradation of the major isoform of the Alzheimer's amyloid peptide, Abeta 1–42, in differentiated PC12 cells. Brain Res. 1997; 746:275–84.10.1016/S0006-8993(96)01262-0 [PubMed: 9037507]

Cano M, Thimmalappula R, Fujihara M, Nagai N, Sporn M, Wang AL, Neufeld AH, Biswal S, Handa JT. Cigarette smoking, oxidative stress, and anti-oxidant response through Nrf2 signaling, and age-related macular degeneration. Vision Res. 2010; 50:652–666.10.1016/j.visres.2009.08.018 [PubMed: 19703486]

Carson JA, Turner AJ. β-Amyloid catabolism: roles for neprilysin (NEP) and other metallopeptidases? J Neurochem. 2002; 81:1–8.10.1046/j.1471-4159.2002.00855.x [PubMed: 12067222]

Carvalho C, Katz PS, Dutta S, Katakam PVG, Moreira PI, Busija DW. Increased susceptibility to amyloid-β toxicity in rat brain microvascular endothelial cells under hyperglycemic conditions. J Alzheimer's Dis. 2014; 38:75–83.10.3233/JAD-130464 [PubMed: 23948922]

Dahlgren KN, Manelli AM, Stine WB Jr, Baker LK, Kraft GA, LaDu MJ. Oligomeric and fibrillar species of amyloid-β peptides differentially affect neuronal viability. J Biol Chem. 2002; 277:32046–32053.10.1074/jbc.M201750200 [PubMed: 12058030]

Dale GE, D'Arcy B, Yuvaniyama C, Wipf B, Oefner C, D'Arcy A. Purification and crystallization of the extracellular domain of human neutral endopeptidase (neprilysin) expressed in *Pichia pastoris*. Acta Crystallogr D Biol Crystallogr. 2000; 56:894–897.10.1107/S0907444900004947 [PubMed: 10930836]

Dasari B, Prasanthi JRP, Marwarha G, Singh BB, Ghribi O. Cholesterol-enriched diet causes age-related macular degeneration-like pathology in rabbit retina. BMC Ophthalmol. 2011; 11:22.10.1186/1471-2415-11-22 [PubMed: 21851605]

Dentchev T, Milam AH, Lee VM, Trojanowski JQ, Dunaief JL. Amyloid-beta is found in drusen from some age-related macular degeneration retinas, but not in drusen from normal retinas. Mol Vis. 2003; 9:184–90. doi: http://dx.doi.org/10.1016/S0002-9394(03)00804-3. [PubMed: 12764254]

Ding J-D, Lin J, Mace BE, Herrmann R, Sullivan P, Bowes Rickman C. Targeting age-related macular degeneration with Alzheimer's disease based immunotherapies: anti-amyloid-β attenuates pathologies in an age-related macular degeneration mouse model. Vision Res. 2008; 48:339–345.10.1016/j.visres.2007.07.025 [PubMed: 17888483]

Ding J-D, Johnson LV, Herrmann R, Farsiu S, Smith SG, Groelle M, Mace BE, Sullivan P, Jamison JA, Kelly U, Harrabi O, Bollini SS, Dilley J, Kobayashi D, Kuang B, Li W, Pons J, Lin JC, Bowes Rickman C. Anti-amyloid therapy protects against retinal pigmented epithelium damage and vision loss in a model of age-related macular degeneration. Proc Natl Acad Sci USA. 2011; 108:E279–E287.10.1073/pnas.1100901108 [PubMed: 21690377]

Dong Z, Li J, Sun X, Hu H, He Y, Tan Z, Ge J. Cyclic intensive light exposure induces retinal lesions similar to age-related macular degeneration in APPswe/PS1 bigenic mice. BMC Neurosci. 2012; 13:34.10.1186/1471-2202-13-34 [PubMed: 22443196]

Edwards MM, Rodríguez JJ, Gutierrez-Lanza R, Yates J, Verkhratsky A, Lutty GA. Retinal macroglia changes in a triple transgenic mouse model of Alzheimer's disease. Exp Eye Res. 2014; 127:252–60.10.1016/j.exer.2014.08.006 [PubMed: 25149907]

Gu L, Guo Z. Alzheimer's Aβ42 and Aβ40 peptides form interlaced amyloid fibrils. J Neurochem. 2013; 126:305–311.10.1111/jnc.12202 [PubMed: 23406382]

Guo L, Salt TE, Luong V, Wood N, Cheung W, Maass A, Ferrari G, Russo-Marie F, Sillito AM, Cheetham ME, Moss SE, Fitzke FW, Cordeiro MF. Targeting amyloid-β in glaucoma treatment. Proc Natl Acad Sci USA. 2007; 104:13444–13449.10.1073/pnas.0703707104 [PubMed: 17684098]

Guo LY, Alekseev O, Li Y, Song Y, Dunaief JL. Iron increases APP translation and amyloid-beta production in the retina. Exp Eye Res. 2014; 129:31–37.10.1016/j.exer.2014.10.012 [PubMed: 25456519]

Hersh LB, Rodgers DW. Neprilysin and amyloid beta peptide degradation. Curr Alzheimer's Res. 2008; 5:225–231.10.2174/156720508783954703

Hetling JR, Pepperberg DR. Sensitivity and kinetics of mouse flash responses determined *in vivo* from paired-flash electroretinograms. J Physiol. 1999; 516:593–609.10.1111/j.1469-7793.1999.0593v.x [PubMed: 10087356]

Hoh Kam J, Lenassi E, Jeffery G. Viewing ageing eyes: diverse sites of amyloid Beta accumulation in the ageing mouse retina and the up-regulation of macrophages. PLoS One. 2010; 5:e13127.10.1371/journal.pone.0013127 [PubMed: 20957206]

Hubin E, van Nuland NAJ, Broersen K, Pauwels K. Transient dynamics of Aβ contribute to toxicity in Alzheimer's disease. Cell Molec Life Sci. 2014; 71:3507–3521.10.1007/s00018-014-1634-z [PubMed: 24803005]

Isas JM, Luibl V, Johnson LV, Kayed R, Wetzel R, Glabe CG, Langen R, Chen J. Soluble and Mature Amyloid Fibrils in Drusen Deposits. Invest Ophthalmol Vis Sci. 2010; 51:1304–1310.10.1167/iovs.09-4207 [PubMed: 19892876]

Itkin A, Dupres V, Dufrene YF, Bechinger B, Ruysschaert J-M, Roussens V. Calcium ions promote formation of amyloid-β-peptide (1–40) oligomers causally implicated in neuronal toxicity of Alzheimer's disease. PLoS ONE. 2011; 6:e18250.10.1371/journal.pone.0018250 [PubMed: 21464905]

Iwata N, Tsubuki S, Takaki Y, Shirotani K, Lu B, Gerard NP, Gerard C, Hama E, Lee HJ, Saido TC. Metabolic regulation of brain Aβ by neprilysin. Science. 2001; 292:1550–2.10.1126/science.1059946 [PubMed: 11375493]

Janciauskiene S, Westin K, Grip O, Krakau T. Detection of Alzheimer peptides and chemokines in the aqueous humor. Eur J Ophthalmol. 2011; 21:104–111.10.5301/EJO.2010.2108 [PubMed: 20602326]

Johnson LV, Leitner WP, Rivest AJ, Staples MK, Radeke MJ, Anderson DH. The Alzheimer's Aβ peptide is deposited at sites of complement activation in pathologic deposits associated with aging and age-related macular degeneration. Proc Natl Acad Sci USA. 2002; 99:11830–11835.10.1073/pnas.192203399 [PubMed: 12189211]

Kummer MP, Heneka MT. Truncated and modified amyloid-beta species. Alzheimer's Res Ther. 2014; 6:28.10.1186/alzrt258 [PubMed: 25031638]

LaFerla FM, Green KN, Oddo S. Intracellular amyloid-β in Alzheimer's disease. Nature Rev Neurosci. 2007; 8:499–509.10.1038/nrn2168 [PubMed: 17551515]

Lee JH, Pidaparti RM, Atkinson GM, Moorthy RS. Design of an implantable device for ocular drug delivery. J Drug Deliv. 2012; 2012:527516.10.1155/2012/527516 [PubMed: 22919500]

Li C, Hersh LB. Neprilysin: assay methods, purification, and characterization. Meth Enzymol. 1995; 248:253–263.10.1016/0076-6879(95)48018-8 [PubMed: 7674925]

Liu C, Cao L, Yang S, Xu L, Liu P, Wang F, Xu D. Subretinal injection of amyloid-β peptide accelerates RPE cell senescence and retinal degeneration. Int J Mol Med. 2015; 35:169–76.10.3892/ijmm.2014.1993 [PubMed: 25385658]

Liu RT, Gao J, Cao S, Cui JZ, Chou CL, Fang E, Matsubara JA. Inflammatory mediators induced by amyloid-beta in the retina and RPE *in vivo*: implications for inflammasome activation in age-related macular degeneration. Invest Ophthalmol Vis Sci. 2013; 54:2225–2237.10.1167/iovs.12-10849 [PubMed: 23462752]

Liu Y, Guan H, Beckett TL, Juliano MA, Juliano L, Song ES, Chow KM, Murphy MP, Hersh LB. In vitro and in vivo degradation of Aβ peptide by peptidases coupled to erythrocytes. Peptides. 2007; 28:2348–2355.10.1016/j.peptides.2007.09.015 [PubMed: 17988763]

Liu Y, Studzinski C, Beckett T, Guan H, Hersh MA, Murphy MP, Klein R, Hersh LB. Expression of neprilysin in skeletal muscle reduces amyloid burden in a transgenic mouse model of Alzheimer's disease. Molec Ther. 2009; 8:1381–1386.10.1038/mt.2009.115 [PubMed: 19471248]

Liu Y, Studzinski C, Beckett T, Murphy MP, Klein RL, Hersh LB. Circulating neprilysin clears brain amyloid. Molec Cell Neurosci. 2010; 45:101–107.10.1016/j.mcn.2010.05.014 [PubMed: 20558294]

Luibl V, Isas JM, Kayed R, Glabe CG, Langen R, Chen J. Drusen deposits associated with aging and age-related macular degeneration contain nonfibrillar amyloid oligomers. J Clin Invest. 2006; 6:378–85.10.1172/JCI25843 [PubMed: 16453022]

Malek G, Johnson LV, Mace BE, Saloupis P, Schmechel DE, Rickman DW, Toth CA, Sullivan PM, Bowes Rickman C. Apolipoprotein E allele-dependent pathogenesis: a model for age-related retinal degeneration. Proc Natl Acad Sci USA. 2005; 102:11900–11905.10.1073/pnas.0503015102 [PubMed: 16079201]

Manzoni C, Colombo L, Bigini P, Diana V, Cagnotto A, Messa M, Lupi M, Bonetto V, Pignataro M, Airoldi C, Sironi E, Williams A, Salmona M. The molecular assembly of amyloid Aβ controls its neurotoxicity and binding to cellular proteins. PLoS ONE. 2011; 6:e24909.10.1371/journal.pone.0024909 [PubMed: 21966382]

Morley JE, Farr SA. The role of amyloid-beta in the regulation of memory. Biochem Pharmacol. 2014; 88:479–485.10.1016/j.bcp.2013.12.018 [PubMed: 24398426]

Nalivaeva NN, Belyaev ND, Zhuravin IA, Turner AJ. The Alzheimer's amyloid-degrading peptidase, neprilysin: can we control it? Internat J Alzheimer's Dis. 2012:Article ID 383796.10.1155/2012/383796

Ning A, Cui J, To E, Ashe KH, Matsubara J. Amyloid-β deposits lead to retinal degeneration in a mouse model of Alzheimer's disease. Invest Ophthalmol Vis Sci. 2008; 49:5136–5143.10.1167/iovs.08-1849 [PubMed: 18566467]

Normando EM, Coxon KM, Guo L, Cordeiro MF. Focus on: amyloid β. Exper Eye Res. 2009; 89:446–447.10.1016/j.exer.2009.05.004 [PubMed: 19464289]

Oakley H, Cole SL, Logan S, Maus E, Shao P, Craft J, Guillozet-Bongaarts A, Ohno M, Disterhoft J, Van Eldik L, Berry R, Vassar R. Intraneuronal beta-amyloid aggregates, neurodegeneration, and neuron loss in transgenic mice with five familial Alzheimer's disease mutations: potential factors in amyloid plaque formation. J Neurosci. 2006; 26:10129–10140.10.1523/JNEUROSCI.1202-06.2006 [PubMed: 17021169]

Oddo S, Caccamo A, Smith IF, Green KN, LaFerla FM. A dynamic relationship between intracellular and extracellular pools of Aβ. Amer J Pathol. 2006; 169:184–194.10.2353/ajpath.2006.050593 [PubMed: 16400022]

Organisciak DT, Vaughan DK. Retinal light damage: mechanisms and protection. Progr Retinal Eye Res. 2010; 29:113–134.10.1016/j.preteyeres.2009.11.004

Park SW, Kim JH, Mook-Jung I, Kim KW, Park WJ, Park KH, Kim JH. Intracellular amyloid beta alters the tight junction of retinal pigment epithelium in 5XFAD mice. Neurobiol Aging. 2014; 35:2013–2020.10.1016/j.neurobiolaging.2014.03.008 [PubMed: 24709310]

Parthasarathy R, Fautsch MP, Pepperberg DR. Quantification of amyloid-beta in mouse and human eye tissues. IOVS. 2014; 2014:35. ARVO E-Abstract 1317.

Pauwels K, Williams TL, Morris KL, Jonckheere W, Vandersteen A, Kelly G, Schymkowitz J, Rousseau F, Pastore A, Serpell LC, Broersen K. Structural basis for increased toxicity of pathological $A\beta_{42}$:$A\beta_{40}$ ratios in Alzheimer's disease. J Biol Chem. 2012; 287:5650–5660.10.1074/jbc.M111.264473 [PubMed: 22157754]

Pikuleva IA, Curcio CA. Cholesterol in the retina: the best is yet to come. Progr Ret Eye Res. 2014; 41:64–89.10.1016/j.preteyeres.2014.03.002

Prakasam A, Muthuswamy A, Ablonczy Z, Greig NH, Fauq A, Rao KJ, Pappolla MA, Sambamurti K. Differential accumulation of secreted AβPP metabolites in ocular fluids. J Alzheimer's Dis. 2010; 20:1243–1253.10.3233/JAD-2010-100210 [PubMed: 20413851]

Pryor NE, Moss MA, Hestekin CN. Unraveling the early events of amyloid-β protein (Aβ) aggregation: techniques for the determination of Aβ aggregate size. Int J Mol Sci. 2012; 13:3038–3072.10.3390/ijms13033038 [PubMed: 22489141]

Puzzo D, Privitera L, Laznik E, Fà M, Staniszewski A, Palmeri A, Arancio O. Picomolar amyloid-β positively modulates synaptic plasticity and memory in hippocampus. J Neurosci 2008. 2008; 28:14537–14545.10.1523/JNEUROSCI.2692-08.2008

Puzzo D, Arancio O. Amyloid-β peptide: Dr. Jekyll or Mr Hyde? J Alzheimer's Dis. 2013; 33:S111–S120.10.3233/JAD-2012-129033 [PubMed: 22735675]

Querfurth HW, LaFerla FM. Alzheimer's disease. New Engl J Med. 2010; 362:329–344.10.1056/NEJMra0909142 [PubMed: 20107219]

Ripoli C, Cocco S, Li Puma DD, Piacentini R, Mastrodonato A, Scala F, Puzzo D, D'Ascenzo M, Grassi C. Intracellular accumulation of amyloid-β (Aβ) protein plays a major role in Aβ-induced alterations of glutamatergic synaptic transmission and plasticity. J Neurosci. 2014; 34:12893–12903.10.1523/JNEUROSCI.1201-14.2014 [PubMed: 25232124]

Roques BP, Noble F, Dauge V, Fournié-Zaluski MC, Beaumont A. Neutral endopeptidase 24.11: structure, inhibition, and experimental and clinical pharmacology. Pharmacol Rev. 1993; 45:87–146. [PubMed: 8475170]

Saido T, Leissring MA. Proteolytic degradation of amyloid β-protein. Cold Spring Harb Perspect Med. 2012; 2:a006379.10.1101/cshperspect.a006379 [PubMed: 22675659]

Selkoe DJ. Preventing Alzheimer's disease. Science. 2012; 337:1488–1492.10.1126/science.1228541 [PubMed: 22997326]

Sharma K, Sharma NK, Anand A. Why AMD is a disease of ageing and not of development: mechanisms and insights. Front Aging Neurosci. 2014; 6:article 151. doi:10:3389/fnagi.2014.00151. [PubMed: 25071560]

Shirotani K, Tsubuki S, Iwata N, Takaki Y, Harigaya W, Maruyama K, Kiryu-Seo S, Kiyama H, Iwata H, Tomita T, Iwatsubo T, Saido TC. Neprilysin degrades both amyloid beta peptides 1–40 and 1–42 most rapidly and efficiently among thiorphan- and phosphoramidon-sensitive endopeptidases. J Biol Chem. 2001; 276:21895–901.10.1074/jbc.M008511200 [PubMed: 11278416]

Solomonov I, Korkotian E, Born B, Feldman Y, Bitler A, Rahimi F, Li H, Bitan G, Sagi I. Zn^{2+}-Aβ40 complexes form metastable quasi-spherical oligomers that are cytotoxic to cultured hippocampal neurons. J Biol Chem. 2012; 287:20555–20564.10.1074/jbc.M112.344036 [PubMed: 22528492]

Soscia SJ, Kirby JE, Washicosky KJ, Tucker SM, Ingelsson M, Hyman B, Burton MA, Goldstein LE, Duong S, Tanzi RE, Moir RD. The Alzheimer's disease-associated amyloid-β-protein is an antimicrobial peptide. PLoS ONE. 2010; 3:e9505.10.1371/journal.pone.0009505 [PubMed: 20209079]

Tanzi RE, Moir RD, Wagner SL. Clearance of Alzheimer's Aβ peptide: the many roads to perdition. Neuron. 2004; 43:605–8.10.1016/j.neuron.2004.08.024 [PubMed: 15339642]

Tao W. Application of encapsulated cell technology for retinal degenerative diseases. Expert Opin Biol Ther. 2006; 6:717–726.10.1517/14712598.6.7.717 [PubMed: 16805711]

Turner AJ, Isaac RE, Coates D. The neprilysin (NEP) family of zinc metalloendopeptidases: genomics and function. Bioessays. 2001; 23:261–269.10.1002/1521-1878(200103)23:3<261::AID-BIES1036>3.0.CO;2-K [PubMed: 11223883]

Walsh DM, Selkoe DJ. Aβ oligomers – a decade of discovery. J Neurochem. 2007; 101:1172–1184.10.1111/j.1471-4159.2006.04426.x [PubMed: 17286590]

Wang J, Zhu C, Xu Y, Liu B, Wang M, Wu K. Development and expression of amyloid-β peptide 42 in retinal ganglion cells in rats. Anat Rec. 2011; 294:1401–1405.10.1002/ar.21438

Wang J, Ohno-Matsui K, Morita I. Elevated amyloid β production in senescent retinal pigment epithelium, a possible mechanism of subretinal deposition of amyloid-β in age-related macular degeneration. Biochem Biophys Res Commun. 2012; 423:73–78.10.1016/j.bbrc.2012.05.085 [PubMed: 22634014]

Warmlander S, Tiiman A, Abelein A, Luo J, Jarvet J, Soderberg KL, Danielsson J, Graslund A. Biophysical studies of the amyloid β-peptide: interactions with metal ions and small molecules. Chembiochem. 2013; 14:1692–1704.10.1002/cbic.201300262 [PubMed: 23983094]

Wildsmith KR, Holley M, Savage JC, Skerrett R, Landreth GE. Evidence for impaired amyloid β clearance in Alzheimer's disease. Alzheimer's Research & Therapy. 2013; 5:33.10.1186/alzrt187

Woodell A, Rohrer B. A mechanistic review of cigarette smoke and age-related macular degeneration. Adv Exper Med Biol. 2014; 801:301–307.10.1007/978-1-4614-3209-8_38 [PubMed: 24664711]

Yankner BA, Lu T. Amyloid-β-protein toxicity and the pathogenesis of Alzheimer disease. J Biol Chem. 2009; 284:4755–4759.10.1074/jbc.R800018200 [PubMed: 18957434]

Yoneda S, Hara H, Hirata A, Fukushima M, Inomata Y, Tanihara H. Vitreous fluid levels of beta-amyloid (1–42) and tau in patients with retinal diseases. Jpn J Ophthalmol. 2005; 49:106–108.10.1007/s10384-004-0156-x [PubMed: 15838725]

Yoon SS, Jo SA. Mechanisms of Amyloid-β Peptide Clearance: Potential Therapeutic Targets for Alzheimer's Disease. Biomol Ther (Seoul). 2012; 20:245–55.10.4062/biomolther.2012.20.3.245 [PubMed: 24130920]

HIGHLIGHTS

1. Intravitreally injected soluble neprilysin (sNEP) reduces Aβ in living mouse eyes.
2. Reductions of both $A\beta_{40}$ and $A\beta_{42}$ increase with sNEP dose.
3. Aβ reductions following sNEP treatment persist for up to 12 weeks.
4. ERG recordings show that sNEP treatment is well-tolerated.

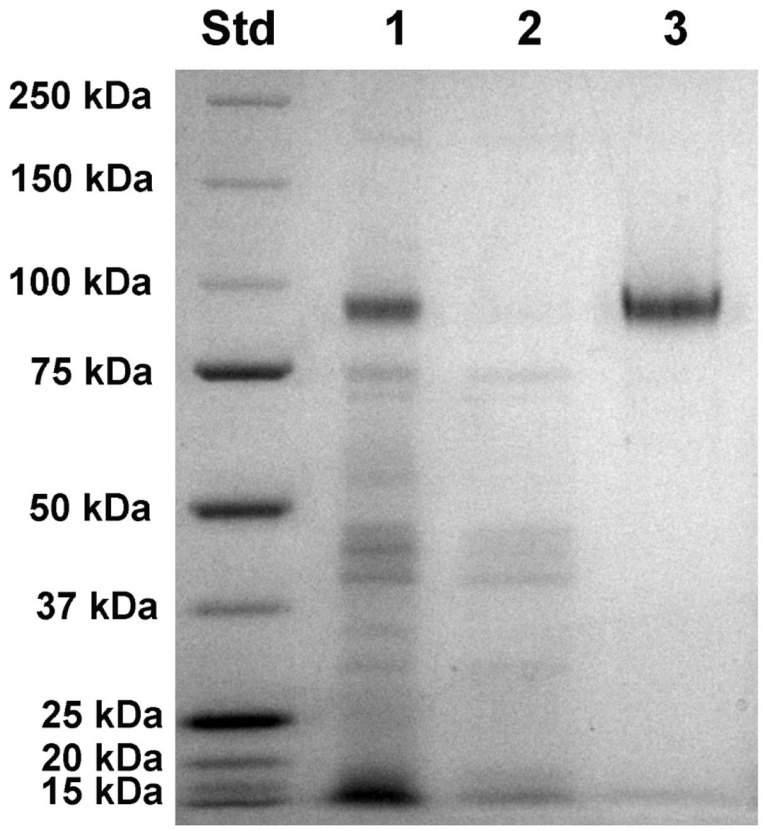

Fig. 1.

SDS-PAGE gel showing the purification of sNEP. The NEP extracellular catalytic domain was expressed as a soluble secreted protein in the *Pichia* expression system. sNEP was purified from conditioned media by first fractionating the conditioned media with ammonium sulfate followed by affinity chromatography on a Ni-NTA column. *Left lane:* molecular weight standards. *Lane 1:* ammonium sulfate fraction. *Lane 2:* flow-through from the Ni-NTA column. *Lane 3:* sNEP eluted from the Ni-NTA column. Protein bands were visualized by Coomassie Blue staining.

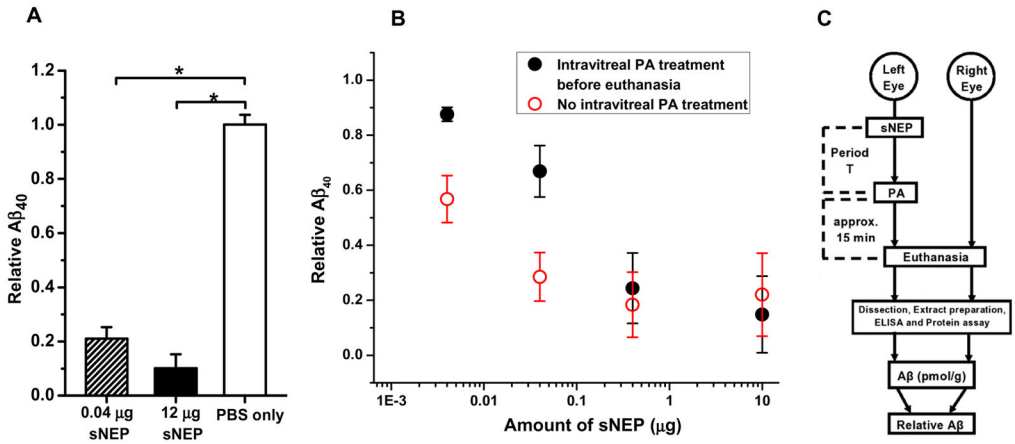

Fig. 2.

$A\beta_{40}$ cleavage in C57BL/6J eyes by intra-vitreally delivered sNEP. **A:** Relative $A\beta_{40}$ at 2 hr post-treatment in mice for which treatment consisted PBS alone (n=2; open bar), 0.04 µg sNEP (n=2; shaded bar), or 12 µg sNEP (n=2; filled bar). Asterisks indicate statistical significance with $p<0.05$. Intra-vitreal delivery of PBS alone (open bar) had no significant effect on relative $A\beta_{40}$ ($p>0.7$). **B:** Results obtained with differing concentrations of delivered sNEP with PA treatment (2 µL of 1 mM PA) (filled circles) and without PA treatment (open circles). Each data point indicates results obtained from $n \geq 3$ animals. **C:** Diagram illustrating the adopted, routine *in vivo* treatment of the test (left) eye and subsequent procedures. "Period T" refers to the post-sNEP-treatment period.

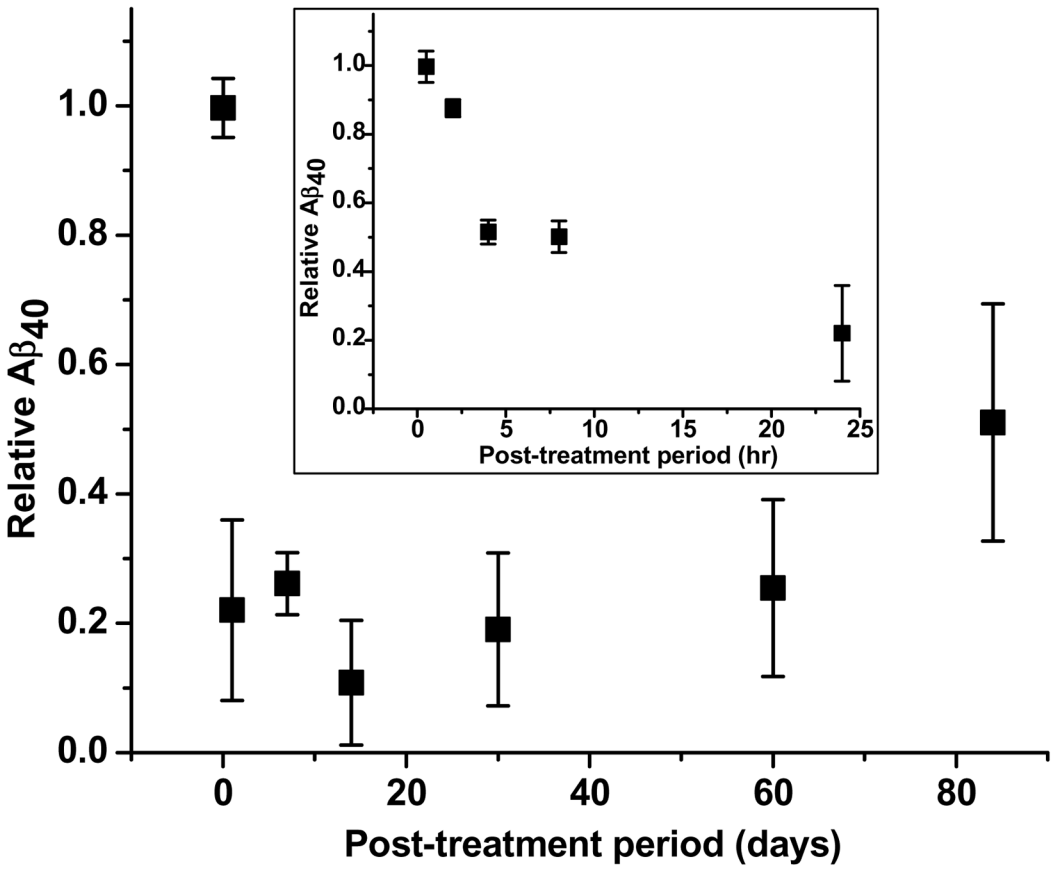

Fig. 3.

Time course of relative $A\beta_{40}$ in sNEP-treated C57BL/6J eyes. Each data point represents results from ≥ 3 animals. The inset shows results obtained with post-treatment periods of 30 min, and 2, 4, 8 and 24 hr. For clarity, the main figure omits the data at 2, 4 and 8 hr. With 30 min and 2 hr post-treatment periods, relative Aβ did not differ significantly from unity ($p>0.05$). However, at 24 hr, relative $A\beta_{40}$ was decreased to 0.22 ± 0.14, and a low level (~0.2–0.3) was maintained with post-treatment periods up to 8 weeks. Relative Aβ determined at 12 weeks post-treatment (0.51 ± 0.18), while less than unity ($p < 0.001$), significantly exceeded that exhibited at 8 weeks (0.25 ± 0.11; $p = 0.01$).

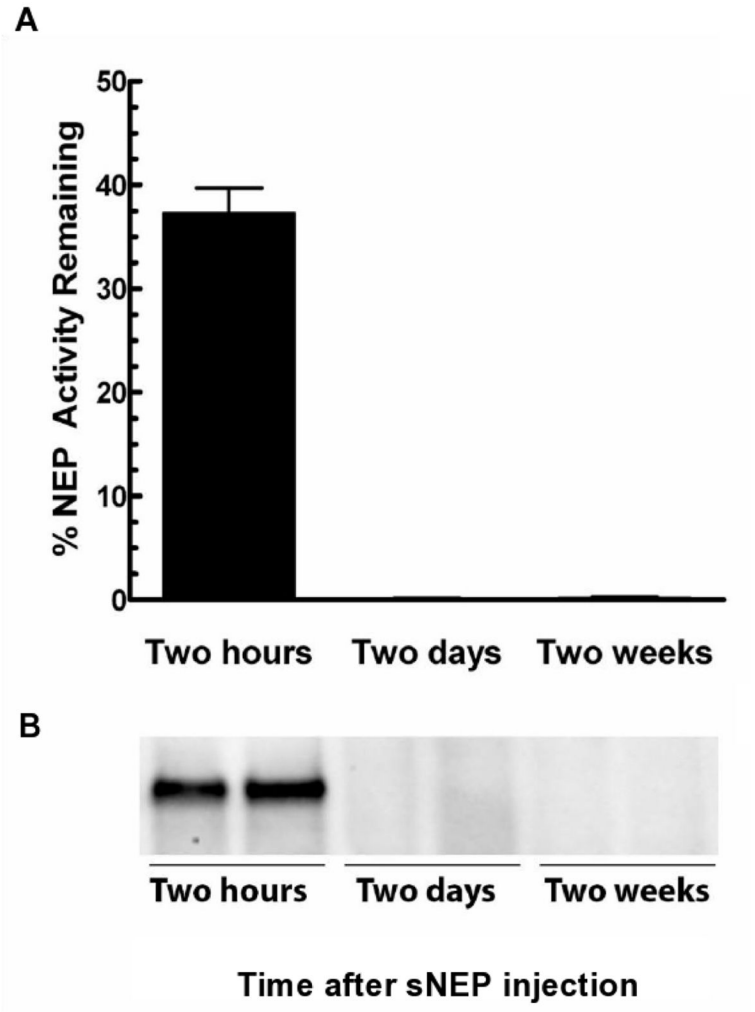

Fig. 4.

Clearance of intra-vitreally delivered sNEP from C57BL/6J eye tissues. Following sNEP treatment, mice were euthanized at the indicated times and eye tissue homogenates obtained. *Top:* Time-dependence of the clearance of sNEP activity as measured in homogenates with G-A-A-F MNA (see Methods). *Bottom:* Time-dependence for the clearance of sNEP immunoreactive protein as measured by Western blot analysis of eye homogenates.

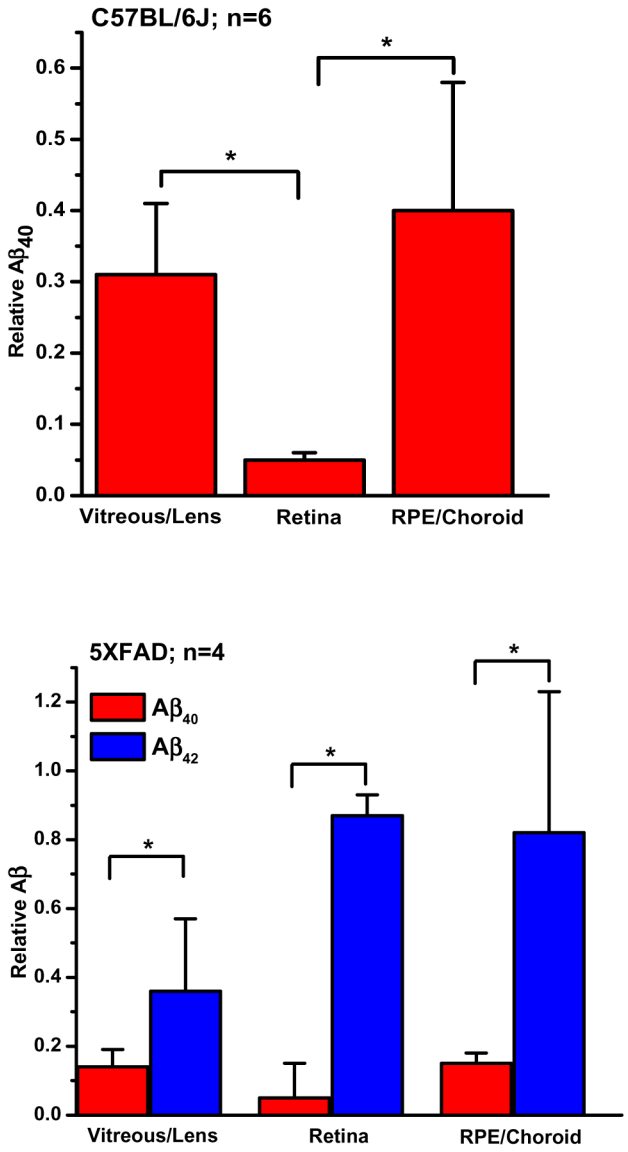

Fig. 5.

Relative Aβ levels determined from separate-tissue extracts. Data from C57BL/6J mice (*top*) and 5XFAD mice (*bottom*) following sNEP treatment (10 μg), 24-hr post-treatment period, and PA addition shortly before euthanasia. Asterisks indicate significant difference with $p < 0.05$.

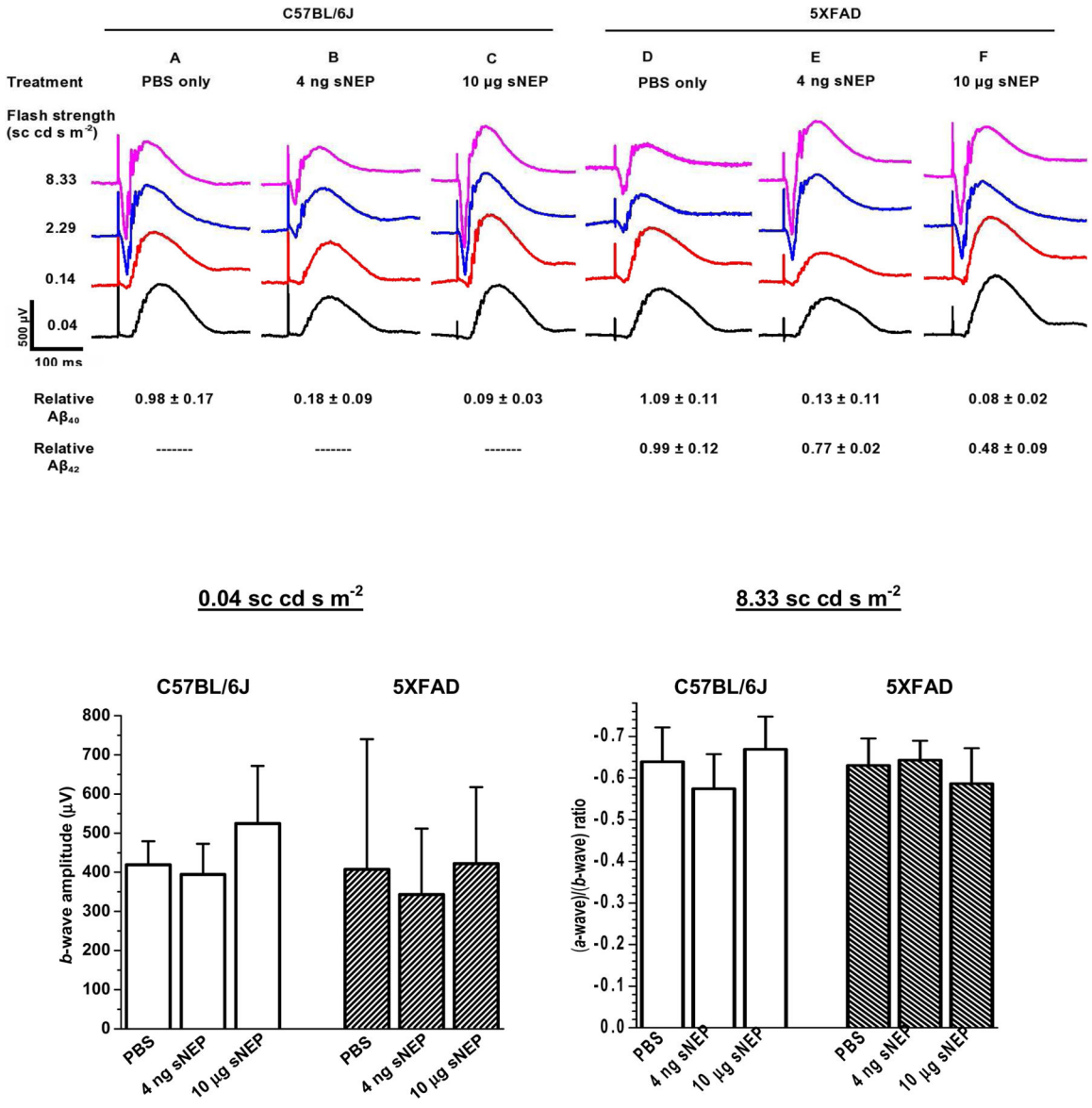

Fig. 6.

ERG responses recorded from eyes of 10-month C57BL/6J mice (columns **A–C**) and 2–3-month 5XFAD mice (columns **D–F**) to a fixed set of test flashes. ERG data were obtained at 9 days following intra-vitreal treatment with PBS alone (**A** and **D**), 4 ng sNEP (**B** and **E**), or 10 µg sNEP (**C** and **F**). Mice were euthanized 2–6 hr after ERG recording. Entries shown in the lower portion of the Figure indicate results obtained for relative $A\beta_{40}$ and $A\beta_{42}$ levels in the treated eyes. Each waveform is the average of 6 responses (3 from each of two identically treated mice) to a flash of the indicated strength. Within the data for a given strain and with a 0.04 sc cd s m^{-2} flash, there were no treatment-dependent significant differences among the *b*-wave amplitude determinations (lower left panel). There were no significant differences among (*a*-wave)/(*b*-wave) amplitude ratios (lower right panel).

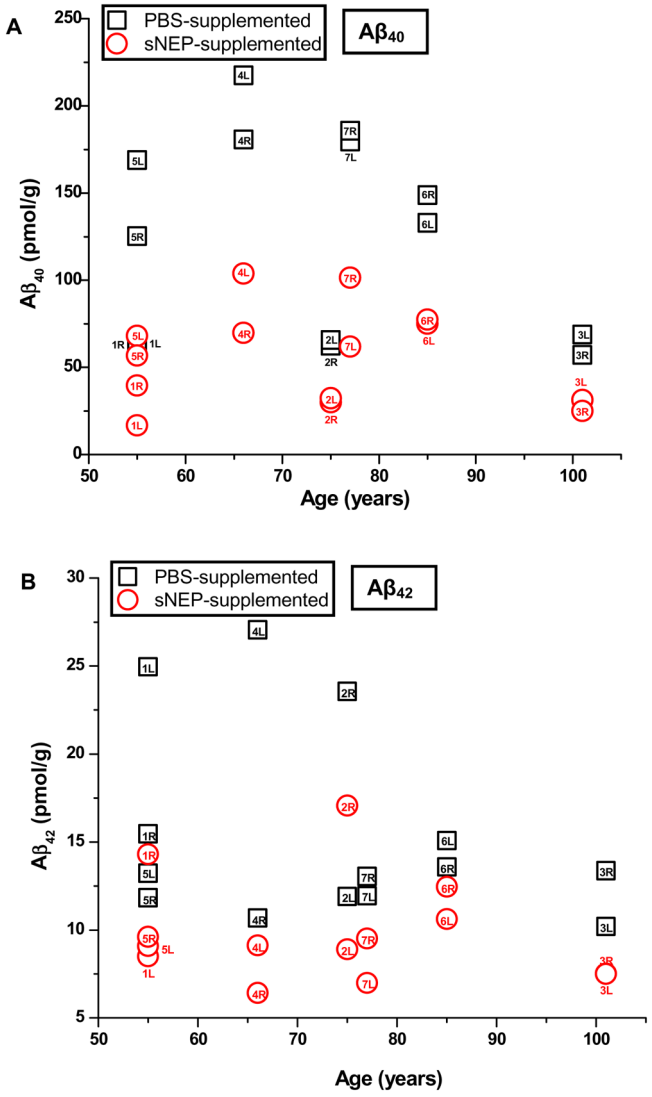

Fig. 7.

Concentrations (pmol/g) of $A\beta_{40}$ (panel **A**) and $A\beta_{42}$ (**B**) determined in PBS-supplemented and sNEP-supplemented vitreous samples (squares and circles, respectively). Labels accompanying each data point indicate donor number and left (L) *vs*. right (R) eye samples.

Table 1

Protein-normalized $A\beta_{40}$ and $A\beta_{42}$ concentrations (mean ± SEM) in combined-tissue extracts of untreated eyes. Extracts from C57BL/6J eyes were not analyzed for $A\beta_{42}$.

Strain	Age (months)	No. of mice	Weight (g)	$A\beta_{40}$ (pmol/g)	$A\beta_{42}$ (pmol/g)
C57BL/6J	2	8	17.6 ± 1.0	2.7 ± 1.3	*
C57BL/6J	10	78	26.2 ± 2.6	42.8 ± 26.3	*
5XFAD	2–3	10	19.5 ± 1.4	73.4 ± 35.5	14.6 ± 8.4

* Extracts of eye tissues from C57BL/6J mice were also tested for $A\beta_{42}$ using a commercial ELISA kit designed for mouse/human $A\beta_{42}$ (product SIG 38956; Covance). However, no significant levels of $A\beta_{42}$ were detected.

Table 2

Relative $A\beta_{40}$ and $A\beta_{42}$ in sNEP-treated eyes of 2–3-month 5XFAD mice.

		Relative level*	
sNEP dose (μg)	**Post-treatment period**	**$A\beta_{40}$**	**$A\beta_{42}$**
10	2 hr	0.11 ± 0.09 (p = 0.01)	0.98 ± 0.10 (p = 0.86)
0.004	1 day	0.38 ± 0.01 (p < 0.001)	0.91 ± 0.27 (p = 0.77)
5	1 day	0.06 ± 0.01 (p < 0.001)	0.53 ± 0.06 (p = 0.02)
10	1 day	0.01 ± 0.01 (p < 0.001)	0.58 ± 0.36 (p = 0.37)
10	3 days	0.03 ± 0.02 (p < 0.001)	0.50 ± 0.03 (p = 0.004)
10	1 month	0.15 ± 0.02 (p < 0.001)	0.45 ± 0.02 (p = 0.001)

*Mean ± SEM of results from ≥ 2 animals. The p value accompanying each entry is the result of two-tailed Student's t-test analysis testing whether the value differs from unity.

Table 3

Protein-normalized Aβ concentrations (mean ± SEM) in extracts of separate compartments of untreated eyes.

Row	Strain	Tissue	$A\beta_{40}$ (pmol/g)	$A\beta_{42}$ (pmol/g)
1	**C57BL/6J** (n=12)	Vitreous/Lens	8.2 ± 2.2	-----
2		Retina	16.2 ± 2.9	-----
3		RPE/Choroid	19.3 ± 3.8	-----
4	**5XFAD** (n=8)	Vitreous/Lens	12.6 ± 4.1	4.3 ± 4.6
5		Retina	17.2 ± 2.5	8.3 ± 5.2
6		RPE/Choroid	31.9 ± 3.1	9.8 ± 3.8

Table 4

Statistical comparison (p-values) of Aβ concentrations (pmol/g protein) determined for the left eye vitreous *vs*. right eye vitreous of human donor eyes.

Donor	p-values	
	$A\beta_{40}$	$A\beta_{42}$
1	0.78	0.40
2	0.67	0.004
3	0.19	0.40
4	0.25	0.40
5	0.06	0.05
6	0.20	0.49
7	0.82	0.51